Geomagnetic activity dependence of O^+ in transit from the ionosphere

W.K. Peterson[1], L. Andersson[1], B. Callahan[1], S.R. Elkington[1], R.W. Winglee[2], J.D. Scudder[3], and H.L. Collin[4].

[1]Laboratory for Atmospheric and Space Physics, University of Colorado, Boulder, 80303
[2]Department of Earth and Space Sciences, University of Washington, Seattle, 98195
[3]Department of Physics and Astronomy, University of Iowa, Iowa City, 52242
[4]Lockheed Martin ATC, B/255, ADCS, 3251 Hanover St., Palo Alto, California 94304
Revised: October 14, 2008

Abstract:

Energetic O^+ ions have important dynamic effects on the ring current. Insights into the effects of O^+ on ring current dynamics have come primarily from models, not observations. Here we discuss observations of O^+ populations escaping from the ionosphere and their access to the plasma sheet and ring current. We review data establishing that a significant flux of O^+ escapes the ionosphere during geomagnetically quiet intervals. We then estimate the relative magnitude of the O^+ population in transit between the ionosphere and ring current during quiet intervals before geomagnetic storms. Our analysis suggests that dynamic reconfigurations of the magnetosphere during geomagnetic storms significantly alter the O^+ transport paths from the ionosphere to the ring current. During these reconfigurations some of the pre-existing, quiet-time, in-transit O^+ populations are captured on magnetic field lines leading to the ring current. The prompt appearance of this O^+ population in the ring current could modify the evolution of the ring current in the storm growth phase. Our analysis suggests that the consequences of an activity-dependent O^+ transport path to the ring current should be systematically investigated.

Keywords: Ionospheric outflow; ring current; plasma sheet; plasma transport

Introduction:

The energetic O^+ population plays an important, but poorly understood, role in ring current development and dynamics. The Earth's ring current was initially thought to be initiated and driven by diffusion processes with little or no pressure or electric field involvement (see, for example, Schulz, 1983). The discovery of the almost instantaneous formation of a new radiation belt in 1991 by Blake et al., [1992] and the subsequent understanding that the radiation belt and ring current are the result of the dynamic interaction between local plasmas and fields (e.g. Li et al., 1993, Wygant et al., 1994, Brandt et al., 2002, and Delcourt, 2002) fundamentally changed our understanding of the ring current region and its dynamics.

Almost all of the ring current plasma comes from the plasma sheet, which in turn comes from the ionosphere and solar wind (For a recent review of the sources and losses of magnetospheric plasma see Hultqvist et al., 1999). Modelers have established he impacts of assumed initial proton distributions, magnetic, and electric fields on the evolution of geomagnetic storm models (See, for example, Ganushkina et al., 2006). Recent reports have established that energetic O^+ in the ring current dynamically alters the distribution of particle and magnetic field pressures during geomagnetic storms [Fok, 2001, Jordanova, 2003, Lemon 2004, Toffoletto, 2003, Zaharia et al., 2006, Chen et al., 2006, 2007, and Khazanov, 2007]. Furthermore, the changing pressure distributions in the ring current modify the structure of large scale-magnetospheric current systems. See, for example, Anderson et al., [2005]. The best empirical model based on ring current O^+ observations [Roeder et al., 2005] does not capture ring current dynamics. Recent global images from space have shown that O^+ injections into the ring current are episodic and related to sub-storms (e.g. Mitchell et al., 2003). Deriving detailed distributions of ring current O^+ from global images is difficult and relies heavily on assumptions derived from global magnetospheric models, which necessarily make assumptions about the ring current O^+ source population in the plasma sheet or equivalently the physics associated with the energization and transport of O^+ to the plasma sheet. (See for example, Perez et al., 2004.)

For the reasons noted above, our understanding of the O^+ component of ring current plasma and its dynamics is based mostly on large-scale models whose assumptions cannot be adequately validated with existing sparse in-situ observations and global ENA image data, as the interpretations of these data are model dependent. In particular, the energetic O^+ population in the ring current can be produced by more than one acceleration and/or transport mechanisms. Knowledge of the nature of transport paths and energization mechanisms of seed populations from the ionosphere to the ring current is essential to understanding ring current dynamics.

Recently Peterson et al., [2008] suggested that the O^+ transport path from the ionosphere to the plasma sheet, and from there on to the ring current is activity dependent. Supporting evidence for this suggestion is primarily episodic and does not include comprehensive observations or model results during both geomagnetically active and quiet times. The purpose of this paper is to begin to explore how to confirm or refute The Peterson et al. suggestion by making quantitative estimates of O^+ in transit from the ionosphere to the plasma sheet and ring current reservoirs during quiet and active geomagnetic conditions.

Ionospheric Source of O^+

Figure 1, reproduced from Yau et al., [1988], shows the average hemispheric outflow of energetic (> 10eV) O^+ observed over a solar cycle obtained from the Dynamics Explorer (DE) -1 satellite as a function of solar and geomagnetic activity indices. It shows that the global outflow of energetic O^+ outflow depends on both solar and geomagnetic activity levels, whereas the global outflow of energetic H^+ outflow depends only on geomagnetic activity levels. The data in Figure 1 were obtained by integrating average outflowing flux values in static invariant latitude/magnetic local time (INVL, MLT) bins organized by geomagnetic and solar activity indices. The outflowing flux levels and magnetic and solar activity dependence of the energetic outflow of H^+ and O^+ shown in Figure 1 have been confirmed from a variety of instruments on the Akebono [Cully et al., 2003], Polar [Lennartsson et al., 2004, Peterson et al., 2006, 2008], and FAST [Andersson et al., 2004, 2005] satellites as well as by an independent analysis of the DE -1 data [Collin et al., 1998]. The Yau et al. [1988] report contains explicit parameterizations of the energetic ion outflow rates as functions of solar ($F_{10.7}$), and geomagnetic (K_P, A_E, and D_{ST}) indices. The parameterization suggests hemispheric outflow rates of energetic (> 10 eV) O^+ ranging from 0.2 kg/s (K_P=0, F_{107}=70) to 110 kg/s (K_P=9, F_{107}=250).

The three year span of data from Polar and one year span of data from FAST do not include enough samples at all local times during very quiet (i.e. $K_P < 1$) intervals to provide a quantitative estimate of the outflow at the most quiet times. However, detectable fluxes of energetic O^+ were observed during the most quiet geomagnetic intervals reported by Yau et al., Collin et al., and Cully et al. from the DE-1 and Akebono satellites.

As noted by Chappell et al., [1987], Yau and André [1997], and others, there are significant thermal components of upflowing H^+ and O^+ that are lost from the ionosphere, which are not included in the energetic outflow rates shown in Figure 1. The source of the thermal outflow, which is below the energy threshold of the energetic ion mass spectrometers on DE -1, FAST, and Polar, is the polar wind. Thermal ion mass spectrometers on DE -1 and Polar were able to obtain episodic samples of the polar wind. These, and other observations have confirmed that the polar wind consists of H^+, He^+ and O^+ and electrons energized by a number of ‘‘non-classical’’ polar wind ion acceleration mechanisms resulting from strong ionospheric convection, enhanced electron and ion temperatures, and escaping atmospheric photoelectrons. (See Yau et al., [2007] for a review of recent polar wind observations.) Observationally it is not always possible to unambiguously separate an energized ‘‘non-polar-wind’’ ion such as a low energy ‘‘cleft ion fountain’’ ion that has convected into a polar wind flux tube from an energized ‘‘polar-wind’’ ion that is accelerated locally by ‘‘non-classical’’ polar-wind ion acceleration mechanisms. This distinction is not important however for the estimates of the outflowing fluxes of O^+ discussed here.

Peterson et al., [2008] have combined observations of energetic O^+ ions obtained in geomagnetically quiet times (D_{ST} > -50) at solar minimum in dynamic boundary coordinates made above the auroral acceleration region with observations of the thermal O^+ component made from the same satellite [Su et al., 1998]. The Peterson et al. and Su et al. data were obtained during perigee passes of the Polar satellite at altitudes of 5,000 –

7,000 km. Table 1 summarizes the escaping hemispheric O^+ fluxes, including the thermal component, and their characteristic energies and velocities reported by Peterson et al., [2008]. The characteristic energy of the escaping flux is derived from the ratio of energy flux to number flux assuming that the thermal flux reported by Su et al., [1998] at 5,000 km is constant over the polar cap and auroral zone and has a uniform characteristic energy of 1 eV. Data are presented in Table 1 for the polar cap, full auroral region, and four magnetic local time quadrants. The energetic O^+ fluxes shown in Table 1 are consistent with those reported by Chappell et al., [1987] and Huddleston et al., [2005] for quiet solar minimum conditions. We note that Chappell et al., and Huddleston et al., assumed that there was no polar wind O^+ component. They also assumed that all of the energized O^+ from the cleft ion fountain was included in the energetic O^+ component.

The O^+ gravitational potential at the 5,000-6,000 km observational range in Table 1 is 5 V, half of the 10 V required energy per charge for escape from the Earth's surface. Thermal and upwelling O^+ fluxes in the ionosphere, which have energies less than 1 eV, have to acquire at lest 5 eV to be detected at 6,000 km. As noted by André and Yau [1997], Lotko [2007], and others, there are many candidate plasma energization processes active in the auroral zone and polar cap that can provide the required energy to O^+. It is beyond the scope of this paper to address the mechanisms responsible for energizing thermal ionospheric O^+. *We note again, that the results of Yau et al., [1988] and Cully et al., [2003] show that some of these processes are active during even the quietest solar and geomagnetic conditions.*

Significant thermal and energetic fluxes of O^+ are found on field lines at all local times during geomagnetically quiet intervals. The auroral oval is narrowest near noon and widest near midnight. In the Holzworth and Meng [1975] representation of the auroral oval, which was used by Peterson et al., [2008] to determine total outflowing fluxes, ~9% of the auroral zone area is in the noon sector, ~47% in the midnight sector, and the remaining area (~44%) in the dawn and dusk sectors. In comparison, the corresponding percentages of outflowing flux in Table 1 are ~20% (0.91/4.6), ~39% (1.8/4.6) and ~41% (1.87/4.6), respectively. The relative intensity per unit area of the outflowing flux in the noon (cusp/cleft) sector is therefore higher than at other local times. Nevertheless, Table 1 shows that only a fraction of the outflowing O^+ comes from the dayside cusp/cleft region. The amount is approximately one third of the energetic (> 15 eV) measured flux and 10% of the estimated total flux.

The outflowing fluxes and characteristic O^+ energies reported for the full energy range in Table 1 are upper limits because the escaping flux of thermal O^+ is not spatially uniform and its characteristic energy is not well determined. Yau et al., [2007] note that several investigators report more intense O^+ polar wind on field lines connected to a sunlight ionosphere. Polar wind characteristic energies derived by Su et al., [1988] at the 5,000-6,000 km altitude range of interest are not comprehensive; the values reported are the average of a small number of observations. The observed upward velocity range reported by Su et al. (0-2 km/sec) corresponds to energies of less than the 1 eV at this altitude, which is the value used in the calculation. We also note that the calculations in Table 1 assume that the upflowing O^+ population is well characterized by one energy value. Nevertheless, the hemispheric outflow rates and characteristic energies reported by Peterson et al., [2008] and summarized in Table 1 are the first to consider both the energetic and thermal components of O^+ in calculating a characteristic energy of escaping

O^+. These observations, when combined with estimates of plasma sheet and ring current O^+ populations reported below allow us to make a quantitative estimate of the 'in-transit' O^+ population in the magnetosphere during quiet geomagnetic conditions before major geomagnetic storms.

In the sections below we estimate the O^+ populations in the quiet time plasma sheet and ring current and compare them to the source rates at solar minimum and solar maximum. This comparison is best done in terms of mass and mass flux. Table 1 shows that 0.3 kg/s (1.1 $x10^{25}$ ions/s) O^+ ions are moving upward at ~6,000 km during quiet geomagnetic intervals characterized by average K_P of 2- and $F_{10.7}$ of 92 [Peterson et al., 2006, 2008]. Yau et al., [1988, eqn. 9] estimate that the quiet-time (K_P =0) O^+ outflow rates are 0.2 and 1.2 kg/s at solar minimum (F_{107} = 70) and maximum (F_{107} = 250), respectively; the disturbed-time (K_P=9) rates are 18 and 110 kg/s at solar minimum and maximum, respectively.

O^+ in the plasma sheet

The plasma sheet is a dynamic plasma reservoir. It contains a variable fraction of O^+ depending on recent solar and geomagnetic activity. See Hultqvist et al., [1999] for a recent review. Figure 2, which is reproduced from Lennartsson and Shelley [1986], shows that for energies above 100 eV, the average O^+ plasma sheet density in the region $10 < R_E < 22$ in the magnetotail varies from ~0.01 to ~ 0.1 cm^{-3} at solar minimum depending on magnetic activity. The data in Figure 2 were obtained from the ISEE -1 spacecraft in 1978 during solar minimum conditions. These data show that at quiet times the Y_{GSM} (dawn/dusk) distribution of O^+ density is low and relatively uniform, whereas at active times it is much higher and peaked near Y_{GSM} = 0. Peterson et al., [2008] suggested that the data in Figure 2 reflect an activity dependent transport path for O^+ between the ionosphere and plasma sheet. Supporting evidence for this suggestion includes observations of significant increases in the flux of escaping O^+ ions from the noon and midnight magnetic local time quadrants during geomagnetically active times (e.g. Strangeway et al., 2005, and Tung et al., 2001) and two recent multi-fluid simulations (Winglee et al., 2008, and Harnett et al., 2008). This supporting evidence is however not conclusive. It is primarily episodic and does not include comprehensive observations or model results during geomagnetically quiet times. The purpose of this paper is to begin to explore how to confirm or refute this suggestion by making quantitative estimates of the quantity of O^+ in transit from the ionosphere to the plasma sheet and ring current reservoirs during quiet times before major geomagnetic storms. In this section we estimate the mass of O^+ in the quiet time plasma sheet.

There is some ambiguity about the existence of a thermal (~ eV) O^+ population in the plasma sheet. The data in Figure 2 were obtained over the energy range 100 eV < E/q < 16 keV with a temporal resolution of ~10 minutes. Chappell et al. [1987] suggested that a significant O^+ population with energies less than 100 eV/e might not be included in Figure 2. Seki et al., [2003] established that there is a significant cold ion population in the hot plasma sheet, but were unable to determine if it was H^+ or O^+. Lennartsson (private communication) argues that if there was a significant thermal (<100 eV/e) O^+ population in the plasma sheet, it would appear above 100 eV (and be evident in his statistical studies) every time the **E**x**B** bulk plasma drift energy was above 100 eV, which corresponds to a velocity of 35 km/s. Recent O^+ observations from Cluster obtained at X_{GSM} ~ -19 R_E by Kistler et al., [2005] show that most of the O^+ density detected by the

Cluster CODIF detector [Réme et al., 1997] above ~40 eV comes from ions with energies above 100 eV. We conclude that the existence of a thermal (i.e. ~ eV) O^+ population in the plasma sheet is possible, but the density of thermal O^+ in the plasma sheet is small compared to that of the energetic components reported by Lennartsson, Kistler, and their co-workers. In the estimates presented here, we assume that the majority of O^+ ions in the plasma sheet and ring current have energies above 20 eV.

Ionospheric ions are energized by a variety of processes between the ionosphere and plasma sheet. In addition, not all of the O^+ ions included in the inventory given in Table 1, reach the plasma sheet. (See, for example, Hulqvist et al.,1999.) The characteristic energy of O^+ in the plasma sheet is significantly larger than it is in the ionosphere or in transit at ~ 6,000 km as noted in Table 1. Lennartsson and Shelley [1986] reported that the characteristic energy of O^+ in the plasma sheet was ~ 4 keV near YGSM =0 and slightly higher (~6 keV) on the flanks of the plasma sheet, independent of geomagnetic activity.

Most investigations of O^+ transport from the auroral source region to the plasma sheet have focused on geomagnetically active times when O^+ can sometimes be the dominant plasma sheet ion. See, for example, Peroomian et al. [2006]. Implicit in these studies is the assumption that nearly all O^+ enters the plasma sheet near the midnight meridian even during quiet times. For example, Cladis (1986) proposed that parallel acceleration on curved dayside magnetic field lines (i.e. centrifugal acceleration) provided the energy that allowed thermal O^+ from the dayside to populate the central plasma sheet during disturbed times. Cully et al., [2003] and Howarth and Yau [2008] have examined the transport of thermal O^+ to the plasma sheet based on data from the

Akebono Suprathermal Mass Spectrometer (SMS). These analyses illustrate the importance of the slow velocity and long transit times of O^+ along field lines compared to the time it takes the magnetosphere to reconfigure during disturbed times. Cully et al., [2003] suggest that the O^+ mass loading during quiet times plays an important role in substorm dynamics. However the focus of this paper is not on substorm dynamics. The focus is on ring current dynamics: especially the magnitude and distribution in space and time of the in transit quiet time O^+ population on ring current evolution. To do this we require knowledge of the magnitude of the O^+ population in the plasma sheet under all conditions.

There are several ways to estimate the O^+ population in the plasma sheet during geomagnetically quiet times. All of them require estimates of the volume and average O^+ density. We want estimates for both solar minimum and solar maximum conditions so we have to consider the data available at solar maximum. Kistler et al., [2006] reported characteristic O^+ densities at ~ $19R_E$ in the plasma sheet of ~ 0.02 cm^{-3} in the quiet intervals before substorms near solar maximum from 2001 to 2004. Yau et al., [1988] estimate that there is about six times more O^+ leaving the ionosphere during quiet times at solar maximum. If all of this extra O+ reaches the plasma sheet and the plasma sheet volume does not change, the plasma sheet density at solar maximum would be 0.06 cm^{-3}. The average O^+ plasma sheet density over its full volume should therefore be in the range from 0.02 to 0.06 cm^{-3}. In the estimates below we use the value 0.04 cm^{-3} for the average O^+ plasma sheet density during geomagnetically quiet times at solar maximum. We assume the quiet time plasma sheet volumes given by Chappell et al., [1987] of 4×10^{24} m^3. Using average O^+ densities of 0.01 (0.04) cm^{-3} for solar minimum (maximum) we obtain the O^+ mass in the plasma sheet of ~1000 (4000) kg for geomagnetically quiet times during solar minimum (maximum). Assuming that the plasma sheet volume is the same during storm and non-storm times and that H^+ and O^+ have comparable number densities independent of solar activity, we obtain ~13,000 kg for the storm time plasma sheet O^+ mass. These are, of course, order-of-magnitude estimates because we don't fully understand plasma sheet dynamics.

O^+ in the Ring current

The ring current, like the plasma sheet, is a dynamic reservoir of O^+. As noted in the introduction, relatively little is known directly from observations about the O^+ population in the ring current and its dynamics. Grande et al., [1997] used data from CRRES to show that increased O^+ in the ring current is associated with the peak phase of substorms (i.e. during intervals of magnetospheric reconfiguration). Korth et al., [2000] used data from CRRES to establish that ring current O^+ ions come from the plasma sheet and not directly from the auroral acceleration region. Korth et al. also established that low energy (<30 keV) ions contribute to the ring current during the main phase of a storm. Li et al., [2003] and others have shown that the known mechanisms driving transport and energization of plasma sheet ions including O^+ to ring current energies are mass independent. However, Pulkkinen et al., [2001] used data from Polar to show that the evolution of the location of flux maxima for ring current H^+ and O^+ were different during geomagnetic storms, and that the increase of O^+ relative to H^+ in the ring current during storms was not as well defined or strong as reported by Yau et al., [1988]. Pulkkinen et al. acknowledged that the slow sampling interval (compared to characteristic times for storms) in their study limited the conclusions they could draw. Nevertheless, they noted that their data suggested new mass dependent selection, energization or transport processes not previously considered.

Here we make quantitative estimates of the ring current O^+ population using the Dessler-Parker-Sckopke (DPS) relation [Dessler and Parker, 1959, Sckopke, 1966] under various solar and geomagnetic conditions. The DPS relation indicates that total ring current energy (in units of keV) is directly proportional to the value of the D_{ST} index (in units of nT). Greenspan and Hamilton [2000] used satellite data from several storms to show that the proportionality constant was approximately 2 x 10^{29} keV/nT. Pulkkinen et al. [2001] showed that the correlation between D_{ST} and energy density does not depend strongly on the relative mass composition.

In the quiet periods before a storm, the relative O^+ content of the ring current is small. Lennartsson and Shelley [1986] report that the source population of the ring current in the plasma sheet has a ~1% ratio of O^+ to H^+ during quiet times at solar minimum. Greenspan and Hamilton [2002] report a similar ratio in the ring current under similar conditions. Pulkkinen et al., [2001] reported O^+/H^+ density ratios of less than 10% during solar minimum. However their analysis included both quiet and active geomagnetic conditions. If we assume that the O^+/H^+ ratio is ~1% in the ring current at quiet times at solar minimum, and that the average energy of the ring current is 40 keV, and use the constant 2 x 10^{29} keV/nT derived by Greenspan and Hamiltion for a D_{ST} value of -40, then the mass of O^+ in the ring current at quiet times during solar minimum given by the DPS relation is ~50 kg. These solar minimum, quiet time, estimates are uncertain because of uncertainties in the quiet time ring current O^+/H^+ flux ratios and relative energy distributions. At quiet times, it is unlikely that the O^+/H^+ flux ratios are greater than 1%. Roeder et al. [2005] have shown that the time averaged (including storm times) ring current O^+ energy spectra are significantly softer than those of H^+. Lower O^+ densities lead to lower ring current masses. In contrast, the DPS relation shows that lower O^+ energies imply larger O^+ ring current masses.

There are even fewer observational constraints on the ring current O^+ mass at solar maximum during quiet times. Plasma sheet composition observations at solar maximum are only available from Cluster in the deep tail. Ring current observations at solar maximum reported by Greenspan and Hamilton [2002], Korth et al. [2000], and Grande et al., [1997] focused on storm time intervals. Here we assume that the O^+/H^+ mass ratio in the ring current is ~1% at quiet-time independent of solar activity and that it increases with the level of geomagnetic activity and the resulting O^+ source rate, as parameterized by Yau et al. [1988]. These assumptions lead to estimates of the solar maximum quiet time ring current O^+ mass at 50 and 300 kg respectively during solar minimum and maximum conditions. The latter number is an overestimate because it implies that all of the enhanced O^+ outflow at solar maximum and none of the enhanced H^+ reach the ring current during quiet times. We use these upper limits in the discussion below.

To understand the dynamics of O^+ in the magnetosphere during storms, we need an estimate of the upper limit to the mass of O^+ in the ring current during storms. Greenspan and Hamilton [2002] examined the relative energy of O^+ and H^+ in the ring current during 67 storms between 1984 and 1990 from the AMPTE/CCE mission. Only 4 of the storms had the O^+/H^+ ratio above 1 and two of these were relatively small storms (D_{ST} ~-100) at solar minimum. Their analysis suggests that at solar maximum ($F_{10.7}$ ~250) the O^+/H^+ energy ratio is ~ 1. If we assume D_{ST} ~-250 and the O^+/H^+ energy ratio of 1, the DPS relation suggests the O^+ content of the storm time ring current is ~4,500 kg independent of geomagnetic activity.

O^+ transport and magnetospheric reconfigurations

In addition to O^+ in the plasma sheet and ring current dynamic reservoirs, there is a significant quantity of O^+ in transit along magnetic field lines throughout the magnetosphere even during geomagnetically quiet intervals. During intervals of magnetospheric reconfigurations associated with changes in the solar wind driving forces, substorms and the onset of geomagnetic storms, the relatively slow moving minority O^+ constituent can be transferred to new field lines and perhaps have more direct access to the ring current. Previous investigations of transport of O^+ from the ionosphere to the ring current have not considered this possibility [e.g. Huddleston et al., 2005, and Ebihara et al., 2006]. In this section we address this problem by making preliminary estimates of the O^+ population in transit during the quiet times before geomagnetic storms and relate them to O^+ in the plasma sheet and ring current reservoirs.

There are at least two simple ways to use the published observational data to estimate the mass of the O^+ population in transit between the ionosphere and ring current during quiet geomagnetic times. Table 1 shows that characteristic velocities of O^+ at 1 R_E are ~ 1/3 R_E/min in the auroral zone and ~1/10 R_E/min in the polar cap. Travel times to the plasma sheet thus range from about a half hour to two hours depending on the specific magnetic field line traversed. A second approach to estimating the in transit O^+ population is based on the data presented in Table 2. Table 2 summarizes the O^+ masses (i.e. quantities of O^+) estimated to be in the plasma sheet and ring current reservoirs during both geomagnetically quiet times and at the peak of relatively large geomagnetic storms (D_{ST} ~ -250) during solar minimum and maximum presented above. It also includes the ionospheric O^+ source rates discussed above and the O^+ mass to source rate ratios; the latter correspond to the minimum possible injection times of the O^+ mass into the plasma sheet and ring current reservoirs. As shown in Table 2, the mass to source rate ratios at quiet times are comparable to the 0.5 to 2 hour transit time estimates based on observed O^+ quiet time velocities at 1 R_E.

To estimate the in-transit O^+ mass at quiet times before storms, we have to consider several other factors. An unknown, and presumably large, fraction of O^+ on the dayside and in the polar cap will be lost from the magnetosphere into the magnetotail, where they have been observed [e.g. Seki et al., 2000]. Additionally an unknown fraction of the upward flowing ionospheric O^+ source flux of 0.2 kg/s at ~6,000 km (2 R_E, geocentric distance) reported by Peterson et al. [2008] will not have the extra 1 to 2 eV of upward directed energy to reach the plasma sheet at 10 R_E and will fall back down to the ionosphere [Howarth and Yau, 2008]. O^+ ions falling back to the ionosphere or continuing down the magnetotail will, however, still be on magnetospheric field lines available for transport to the ring current during magnetospheric reconfigurations and are thus part of the in-transit O^+ population the size of which we want to estimate. Estimates of the returning O^+ population require detailed trajectory calculations such as those done by Huddleston et al., [2005] and Howarth and Yau [2008]. So do estimates of how deep in the magnetotail O^+ on open field lines during quiet times can be and still be incorporated onto closed field lines leading to the ring current during reconfigurations of the magnetosphere. Such detailed trajectory calculations are beyond the scope of this report. Our objective here is to estimate the in-transit O^+ population and compare its magnitude to that in the quiet time plasma sheet and ring current reservoirs.

The O^+ losses into the deep magnetotail and ionosphere have the practical effect of increasing the in-transit time estimated from the simple mass injection time ratios in Table 2. We can therefore say that the mass of O^+ flowing out of the ionosphere during the 0.5 to 2 hr estimate of the transit time based on the assumption that there are no losses to the deep tail or ionosphere is a lower limit to the mass of in-transit O^+. Taking one hour as the lower limit for the characteristic transit time for ionospheric ions to reach the plasma sheet implies that 0.2 (1.2) kg/s x 3600 s = 720 (4300) kg of O^+ are on magnetospheric field lines during the quiet times before magnetic storms at solar minimum (maximum).

Discussion and conclusions

Modelers have explored the impacts of assumed initial proton distributions, magnetic, and electric fields on the evolution of geomagnetic storm models. Here we focus on the role of O^+. The consequences of activity-dependent O^+ transport paths to the plasma sheet and beyond to the ring current have just begun to be explored in magnetospheric models. Huddleston et al., [2005], Ebihara et al., [2006], and others have used models to explore the transport of O^+ from the ionosphere to the ring current based on average properties of thermal ion outflow. These analyses are based on static magnetic field configurations and do not include the effects of O^+ transfers between field lines during dynamic reconfigurations of the magnetosphere in the build up of large geomagnetic storms. The objective here is to estimate the in-transit O^+ population and compare its magnitude to that in the quiet time plasma sheet and ring current reservoirs to determine if more extensive modeling work is justified.

At non-storm times, we estimate that the in-transit O^+ population is > 720 (4300) kg at solar minimum (maximum). This mass is comparable to the estimated plasma sheet O^+ mass and significantly larger than the estimated ring current O^+ mass given in Table 2. We note here that the data in Table 2 also confirms that access of O^+ to the ring current is significantly impeded during geomagnetically quiet times and less so during storm times. We also note that an unknown fraction of the in-transit O^+ is on field lines that, during magnetospheric reconfigurations associated with storms and substorms, provide direct access for O^+ to reach the plasma sheet. We conclude that further modeling of O^+ transport in dynamic field models is justified to determine the possible importance of the in-transit O+ population in the initiation of large geomagnetic storms.

Table 2 shows that the O^+ ring current mass to source rate ratio during storm times is comparable to that during non-storm times, and that it is just a few minutes. This low ratio reflects the relatively direct access of ionospheric O^+ to the ring current at the maxima of large geomagnetic storms. Other investigators (e.g. Korth et al., 2000) have shown that the O^+ path from the ionosphere to the ring current goes through the plasma sheet. The relatively lower ratio of plasma sheet O^+ mass to source rate during storms is consistent with more efficient transmission of O^+ through the plasma sheet to the ring current during the maxima of large geomagnetic storms. We also note that the one hour time scale and other assumptions used to estimate the storm time O^+ populations (K_P=9, D_{ST}= -250) give extremely large estimates for the in-transit population: > 65,000 (400,000) kg during solar minimum (maximum). The quiet time in-transit O^+ population, under the assumption of a one-hour time scale (K_P=0, D_{ST}= -40), is 720 (4,300) kg during solar minimum (maximum).

We have not considered ring current loss processes above because we don't have comprehensive observations or simple first principle models to use to estimate the O^+ mass loss rates. The relative loss rates of H^+ and O^+ during and after the main phase of geomagnetic storms have been investigated but the results are ambiguous because of the lack of comprehensive mass-resolved data and robust models [e.g., Hultqvist et al., 1999, Keika et al., 2006]. We also now understand that the asymmetric component of the ring current plays an important role in storm dynamics. A large fraction of O^+ in the asymmetric ring current should leave the magnetosphere through the dayside magnetopause, but the only comprehensive measurements of O^+ in this region are thermal, below the energy range of interest [e.g. Chen and Moore, 2006]. Perhaps the comprehensive and sensitive energetic ion mass spectrometers on NASA's Magnetospheric Multi-Scale (MMS) satellite will be able to characterize the flux of energetic O^+ flowing out the dayside magnetopause well enough to be included in the inventory presented here.

In summary, our analysis suggests that, in the magnetospheric reconfigurations associated with the growth phase of large geomagnetic storms, pre-existing O^+ in the flanks of the plasma sheet in combination with a significant pre-existing O^+ population in-transit to the plasma sheet and in the magnetospheric lobes is energized and transported to the ring current. Our analysis is not conclusive because of its qualitative nature. We suggest that further analysis and modeling addressing how the pre-existing, quiet-time, in-transit O^+ population responds to reconfigurations of the Earth's magnetosphere at the beginning of large geomagnetic storms is justified.

Acknowledgements

WKP thanks Andrew Yau, Mike Schultz, and Tuija Pulkkinen for helpful comments. The research at the University of Colorado was supported by NASA Grant NNX08AF39G.

References

Anderson, B. J., S.-I. Ohtani, H. Korth, and A. Ukhorskiy (2005), Storm time dawn-dusk asymmetry of the large-scale Birkeland currents, J. Geophys. Res., 110, A12220, doi:10.1029/2005JA011246.

Andersson, L., W.K. Peterson, and K.M. McBryde (2004), Dynamic coordinates for auroral ion outflow, *J. Geophys. Res.,* 109, A08201, doi: 10.1029/2004JA010424.

Andersson, L., W.K. Peterson, and K.M. McBryde (2005), Estimates of the suprathermal O^+ outflow characteristic energy and relative location in the auroral oval, *Geophys. Res. Lett., 32*, L09104, doi:10.1029/2004GL021434.

André, Mats and Andrew Yau (1997), Theories and observations of ion energization and outflow in the high latitude magnetosphere, *Space. Sci. Rev*. 80, 27-48.

Blake, J. B., W. A. Kolasinski, R. W. Fillius and E. G. Mullen (1992), Injection of electrons and protons with energies of tens of MeV into L<3 on 24 March 1991", *J. Geophys. Res.,19*, 821.

Brandt, P. C:son, et al. (2002), Global ENA observations of the storm main phase ring current: Implications for skewed electric fields in the inner magnetosphere, *Geophys. Res. Lett.,* 29, 1954, doi:10.1029/2002GL015160.

Chappell, C. R., T. E. Moore, and J. H. Waite Jr. (1987), The Ionosphere as a Fully Adequate Source of Plasma for the Earth's Magnetosphere, *J. Geophys. Res.*, *92*(A6), 5896–5910.

Chen, M. W., S. Liu, M. Schulz, J. L. Roeder, and L. R. Lyons (2006), Magnetically self-consistent ring current simulations during the 19 October 1998 storm, *J. Geophys. Res.*, *111*, A11S15, doi:10.1029/2006JA011620.

Chen, M., C.-P. Wang, M. Schulz, and L. R. Lyons (2007), Solar-wind influence on MLT dependence of plasma sheet conditions and their effects on storm time ring current formation, *Geophys. Res. Lett.*, 34, L14112, doi:10.1029/2007GL030189.

Chen, S.-H., and T. E. Moore (2006), Magnetospheric convection and thermal ions in the dayside outer magnetosphere, *J. Geophys. Res*., 111, A03215, doi:10.1029/2005JA011084.

Cladis, J.B. (1986), Parallel acceleration and transport of ions from the polar ionosphere to the plasmasheet, *Geophys. Res. Lett.* 13, 893.

Collin, H.L., W.K. Peterson, J.F. Drake, and A.W. Yau (1988), The Helium Components of Energetic Terrestrial Ion Upflows: Their Occurrence, Morphology, and Intensity, *J. Geophys. Res.* 93, 7558.

Cully, C. M., E. F. Donovan, A. W. Yau, and H. J. Opgenoorth (2003), Supply of thermal ionospheric ions to the central plasma sheet, *J. Geophys. Res.*, 108, 1092, doi:10.1029/2002JA009457.

Delcourt, D.C. (2002), Particle acceleration by inductive electric fields in the inner magnetosphere, *J. Atmos. and Solar-Terr. Phys.* 64, 551.

Dessler, A . J., and E. N. Parker (1959), Hydromagnetic theory of geomagnetic storms, J. Geophys Res. ,64, 2239-2252.

Ebihara, Y., M. Yamada, S. Watanabe, and M. Ejiri (2006), Fate of outflowing suprathermal oxygen ions that originate in the polar ionosphere, *J. Geophys. Res.*, 111, A04219, doi:10.1029/2005JA011403.

Fok, M.-C., R. A. Wolf, R. W. Spiro, and T. E. Moore (2001), Comprehensive computational model of Earth's ring current, *J. Geophys. Res.*, 106, 8417.

Ganushkina, N.Y., T.I. Pulkkinen, A. Milillo, and M. Liemohn (2006), Evolution of the proton ring current energy distribution during 21-25 April 2001 storm, J. Geophys. Res. 111, A11S08, doi:1029/2006JA011609.

Grande, M, C.H. Perry, A. Hall, J. Fennell, and B. Wilken (1997), Survey of ring current composition during magnetic storms, *Adv. Space Res*., 20, 321.

Greenspan, M.E., and D.C. Hamilton (2000), A test of the Dessler-Parker-Sckopke relation during magnetic storms, J. Geophys. Res. 105, 5419.

Greenspan, M.E. and D.C. Hamilton (2002), Relative contributions of H^+ and O^+ to the ring current energy near magnetic storm maximum, J. Geophys. Res., 107, 1043, doi:10.1029/2001JA0001555.

Harnett, E.M. R.M. Winglee, A Stickle, and Gang Lu, Prompt ionospheric/magnetospheric responses October 29, 2003 Halloween storm: Outflow and energization, to appear in *J. Geophys. Res*., 2008.

Holzworth, R. H., and C.-I. Meng (1975), Mathematical Representation of the Auroral Oval, *Geophys. Res. Lett.* 2, 377.

Howarth, Andrew, and Andrew W. Yau (2008), The effects of IMF and convection on thermal ion outflow in magnetosphere- ionosphere coupling, to appear in *J. Atmos. Solar Terr. Phys*.

Huddleston, M. et al. (2005), An examination of the process and magnitude of ionospheric plasma supply to the magnetosphere, *J. Geophys. Res.*, 110, A12202, doi:10.1029/2004JA010401.

Hultqvist, B., M. Øieroset, G. Pashman and R. Treuman, Editors, *Magnetospheric Plasma Sources and Losses,* Kluwer Academic Publishers, Dordrecht, Boston, London, 1999.

Jordanova, Vania K., New insights on geomagnetic storms from model simulations using multi-spacecraft data, *Space Science Rev.* 107, 157, 2003.

Keika, K., et al., (2006), Contribution of charge exchange loss to the storm time ring current decay: IMAGE/HENA observations, *J. Geophys. Res*., 111, A11S12, doi:10.1029/2006JA011789.

Khazanov, G. V., et al. (2007), Self-consistent model of magnetospheric ring current and propagating electromagnetic ion cyclotron waves: 2. Wave-induced ring current precipitation and thermal electron heating, *J. Geophys. Res. 112,* A04209, doi:10.1029/2006JA012033.

Kistler, L. M., et al. (2005), Contribution of nonadiabatic ions to the cross-tail current in an O^+ dominated thin current sheet, *J. Geophys. Res.*, 110, A06213, doi:10.1029/2004JA010653.

Kistler, L. M., et al. (2006), Ion composition and pressure changes in storm time and nonstorm substorms in the vicinity of the near-Earth neutral line, *J. Geophys. Res.,* 111, A11222, doi:10.1029/2006JA011939.

Korth, A., et al. (2000), Comprehensive particle and field observations of magnetic storms at different local times from the CRRES spacecraft, *J. Geophys. Res*., 105, 18729.

Lemon, C., et al. (2004), Magnetic storm ring current injection modeled with the Rice Convection Model and a self-consistent magnetic field, *Geophys. Res. Lett.,* 31, L21801, doi:10.1029/2004GL020914.

Lennartsson, W., and E. G. Shelley (1986), Survey of 0.1- to 16-keV/*e* Plasma Sheet Ion Composition, *J. Geophys. Res.*, *91*(A3), 3061–3076.

Lennartsson, O.W., W.K. Peterson, and H.L. Collin (2004), Solar wind control of Earth's H^+ and O^+ outflow rates in the 15-eV to 33-keV energy range, *J. Geophys. Res.*, 109, A12212 10.1029/2004JA010690.

Li, Xinlin, et al. (1993), Simulation of the prompt energization and transport of radiation belt particles during the March 24, 1991 SSC, *Geophys. Res. Lett.* 20, 2423.

Li, Xinlin, T.E. Sarris, D.N. Baker, W.K. Peterson, and H.J. Singer (2003), Simulation of energetic particle injections associated with a substorm on August 27, 2001, *Geophys. Res. Lett.* 30, 1004, doi:10.1029/2002GL015967.

Perez, J. D., X.-X. Zhang, P. C:son Brandt, D. G. Mitchell, J.-M. Jahn, and C. J. Pollock (2004), Dynamics of ring current ions as obtained from IMAGE HENA and MENA ENA images, *J. Geophys. Res.*, 109, A05208, doi:10.1029/2003JA010164.

Peroomian, V., M. El-Alaoui, M. Abdalla, and L. Zelenyi (2006), The access of dayside ionospheric O^+ ions to the plasmasheet during the September 24–25, 1998 magnetic storm, *Adv. Space Res.* 28, 1615.

Peterson, W.K., H.L. Collin, O.W. Lennartsson and A.W. Yau (2006), Quiet time solar illumination effects on the fluxes and characteristic energies of ionospheric outflow, *J. Geophys. Res.*, 111, A11S05, doi:10.1029/2005JA011596.

Peterson, W.K., H.L. Collin, O.W. Lennartsson and A.W. Yau (2006), Quiet time solar illumination effects on the fluxes and characteristic energies of ionospheric outflow, *J. Geophys. Res.*, 111, A11S05, doi:10.1029/2005JA011596.

Peterson et al. (2008), Solar-minimum quiet-time ion energization and outflow in dynamic boundary related coordinates, *J. Geophys. Res. 113, A07222, doi:10.1029/2008JA013059.*

Pulkkinen, T.I, et al. (2001), Ring current ion composition during solar minimum and rising solar activity: Polar/Cammice/MICS results, J. Geophys. Res., 106, 19131.

Rème, H., et al. (1997), The Cluster ion spectrometry (CIS) experiment, *Space Sci. Rev.* 79, 303.

Roeder, J. L.,M.W. Chen, J. F. Fennell, and R. Friedel (2005), Empirical models of the low-energy plasma in the inner magnetosphere, *Space Weather,* 3, S12B06, doi:10.1029/2005SW000161.

Schulz, M. (1983), Principles of magnetospheric ion composition, in. *Energetic Ion Composition in the Earth's Magnetosphere,* R.G. Johnson, Editor, Terra Scientific Publishing, Tokyo.

Sckopke, N. (1966), A general relation between the energy of trapped particles and the disturbance field near the Earth, *J Geophys Res.,* 71, 3125-3130.

Seki, K., et al. (2000), Cold flowing O^+ beams in the lobe/mantel at Geotail: Does FAST observe the source?, J. Geophys. Res. 105, 15931.

Seki, Kanako, et al. (2003), Cold ions in the hot plasma sheet of Earth's magnetotail, *Nature*, 422, 589.

Strangeway, R. J., R.E. Ergun. Y.-J. Su. C.W. Carlson, and R.C. Elphic (2005), Factors controlling ionospheric outflows as observed at intermediate altitudes, *J. Geophys. Res.* 110, A03221, Doi: 10.1029/2004JA010829.

Su, Y.J., Horwitz, J.L., Moore, T.E., Giles, B.L., Chandler, M.O., Craven, P.D., Hirahara, M., Pollock, C.J., (1998) Polar wind survey with the thermal ion dynamics experiment/plasma source instrument suite aboard POLAR. *J. Geophys*. Res., 103, 29305–29337.

Toffoletto, F. R., S. Sazykin, R. W. Spiro, and R. A. Wolf (2003), Modeling the inner magnetosphere using the Rice Convection Model, *Space Sci. Rev. 107,* 175.

Tung et al. (2001), Auroral polar cap boundary ion conic outflow observed on FAST, *J. Geophys. Res*., 106, 3603.

Winglee, R.M., W.K. Peterson, A.W. Yau, E. Harnett, and A. Stickle (2008), Model/data comparisons of ionospheric outflow as a function of invariant latitude and magnetic local time, to appear in *J. Geophys. Res*.

Wygant, J., F. et al. (1994), Large amplitude electric and magnetic field signatures in the inner magnetosphere during injection of 15 MeV electron drift echoes, *Geophys. Res. Lett*. 21, 1739.

Yau, A.W., W.K. Peterson, and E.G. Shelley (1988), Quantitative Parameterization of Energetic Ionospheric Ion Outflow, in *Modeling Magnetospheric Plasma*, Geophysical Monograph 44, American Geophysical Union, Washington, DC. 211.

Yau, A.W., T. Abe, and W.K. Peterson (2007), The polar wind: Recent observations, *J. Atoms. Sol. Terr. Phys.*, 69, 1936.

Zaharia, S., V. K. Jordanova, M. F. Thomsen, and G. D. Reeves (2006), Self-consistent modeling of magnetic fields and plasmas in the inner magnetosphere: Application to a geomagnetic storm, *J. Geophys. Res.*, 111, A11S14, doi:10.1029/2006JA011619.

Figures captions

Figure 1. Reproduced From Yau et al., [1988], see text.

Figure 2. Reproduced from Lennartsson and Shelley [1986]. O^+ density in the plasma sheet ($-10 < X_{GSM} < -22\ R_E$, and $|Z_{GSM}| < 7.5\ R_E$) at quiet (dashed lines) and active (solid lines) times.

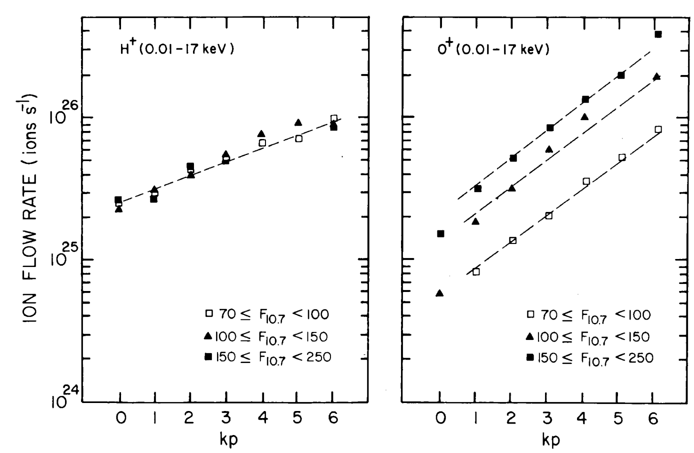

ION FLOW RATE (ions s^{-1})
10^{26}
10^{25}
10^{24}
H$^+$ (0.01 - 17 keV)
O$^+$ (0.01 - 17 keV)
$70 \leq F_{10.7} < 100$
$100 \leq F_{10.7} < 150$
$150 \leq F_{10.7} < 250$
0 1 2 3 4 5 6
kp

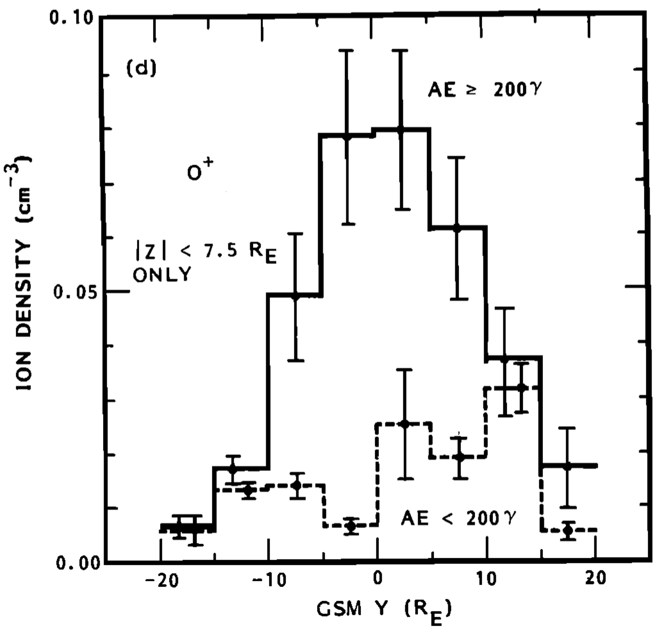

(d)
AE ≥ 200γ
O+
|Z| < 7.5 RE
ONLY
AE < 200γ
ION DENSITY (cm-3)
0.10
0.05
0.00
-20
-10
0
10
20
GSM Y (RE)

Tables

Quantity	Energy Range	Auroral Region	Noon	Dusk	Midnight	Dawn	Polar Cap
Flux	> 15 eV	1.7	0.67	0.18	0.46	0.40	0.05
Flux	Full	4.6	0.91	0.77	1.8	1.1	6.2
Energy	> 15 eV	300	120	330	590	170	190
Energy	Full	100	90	80	150	60	8
Velocity	Full	0.3	0.3	0.3	0.4	0.4	0.1

Table 1: Summary of observations of hemispheric outflow rates of energetic and thermal O^+ and characteristic energies and velocities observed at ~ 6,000 km from the Polar satellite during solar minimum at geomagnetically quiet times reported by Peterson et al. [2008]. Escaping number flux is reported in units of 10^{24} s^{-1}. The characteristic energy and velocity of the escaping flux is derived from the ratio of energy flux to number flux assuming that the thermal flux is constant over the polar cap and auroral zone and has a uniform characteristic energy of 1 eV. Energy is given in units of electron volts (eV). Velocity is given in units of R_E/min assuming a field-aligned population.

Geomagnetic Activity	Variable	Reservoir			
		Plasma Sheet		Ring Current	
	Solar Activity	Minimum	Maximum	Minimum	Maximum
Quiet Times	O^+ mass (kg)	1000	4,000	50	300
	Source rate (kg/s)	0.2	1.2	0.2	1.2
	O^+ mass / source rate (minutes)	80	60	4	4
Storm Times	O^+ mass (kg)	27,000	27,000	4,500	4,500
	Source rate (kg/s)	18	110	18	110
	O^+ mass / source rate (minutes)	25	4	4	1

Table 2: Estimated O^+ reservoir masses (kg) and source rates (kg/s), and mass-to-source-rate ratios (minutes) for various solar and geomagnetic activity conditions. See text.